The Baldwin-Lomax Turbulence Model for Two-Dimensional Shock-Wave/Boundary-Layer Interactions

M. Visbal* and D. Knight†
Rutgers University, New Brunswick, New Jersey

The algebraic turbulent eddy viscosity model of Baldwin and Lomax has been critically examined for the case of two-dimensional (2-D) supersonic compression corner interactions. The flowfields are computed using the Navier-Stokes equations together with three different versions of the Baldwin-Lomax model, including the incorporation of a relaxation technique. The turbulence models are evaluated by a detailed comparison with available experimental data for compression ramp flows over a range of corner angle and Reynolds number. The Baldwin-Lomax outer formulation is found to be unsuitable for separated 2-D supersonic interactions due to the unphysical streamwise variation of the computed length scale in the vicinity of separation. Minor modifications are proposed to partially remedy this difficulty. The use of relaxation provides significant improvement in the flowfield prediction upstream of the corner. However, the relaxation length required is one-tenth of that employed in a previous computational study. All of the turbulence models tested here fail to simulate the rapid recovery of the boundary layer downstream of reattachment.

I. Introduction

THE numerical solution of the Navier-Stokes equations for complex aerodynamic flows is now possible as a result of increases in computer capability, the development of efficient numerical algorithms,[1,2] and the recent advances in grid generation techniques.[3] Practical high-speed flows, however, are usually turbulent and thus a suitable empirical turbulence model must be selected. Algebraic eddy viscosity models still represent the most common choice for compressible Navier-Stokes codes since their implementation results in the minimum requirements of computer time and storage, which is particularly important in three-dimensional (3-D) computations.

Several two-layer algebraic turbulence models (such as Cebeci-Smith[4]) require, for their implementation, the determination of the boundary-layer thickness and edge velocity. This constitutes a practical disadvantage in the numerical solution of the Navier-Stokes equations. Specifically, two effects complicate any attempt to devise a suitable algorithm for determination of the boundary-layer edge, namely, 1) the presence of nonuniform inviscid regions in which the inviscid flow varies in the direction normal to the boundary, and 2) the presence of small spurious oscillations in the numerical solution. As discussed by Hung and MacCormack[5] for compression corner flows and Baldwin and Lomax[6] for transonic flow over an airfoil, large variations in the computed outer eddy viscosity can occur as a result of the uncertainties in the boundary-layer thickness.

In an attempt to overcome this difficulty, Baldwin and Lomax[6] recently proposed a new algebraic eddy viscosity model, patterned after that of Cebeci and Smith. This new model does not require the determination of the boundary-layer edge, and therefore eliminates a source of potential error in the computed outer eddy viscosity. In addition, since it employs the vorticity which is invariant under coordinate transformations, the model may be applied to 3-D configurations.

Due to the above advantages and ease of implementation, the Baldwin-Lomax model is a popular algebraic eddy viscosity model in computational aerodynamics. Indeed, this model has been applied (sometimes quite uncritically) to a variety of 2-D and 3-D flowfield calculations (see, for example, Refs. 7-10). Baldwin and Lomax[6] evaluated their model in detail for the case of transonic flow over an isolated airfoil. Hung[11] employed the Baldwin-Lomax model (in its original form) for the simulation of several compression corner flows. Degani and Schiff[12] recently applied the Baldwin-Lomax model in the computation of supersonic flows around cones at high incidence. They found the model to be unsuitable for regions of cross-flow separation, due to ambiguities in the determination of the length scale. Despite its increasing use, no additional evaluations of the Baldwin-Lomax model have been conducted and are therefore needed. The present investigation is aimed at partially fulfilling this need by performing a critical examination of the Baldwin-Lomax model for the case of shock/boundary-layer interaction in a supersonic compression ramp (Fig. 1). This work represents a more detailed and extensive evaluation than that of Ref. 11. The major focus of this research is to identify the merits and deficiencies of the Baldwin-Lomax model for supersonic interactions, and to develop, when possible, simple modifications (within the limitations of the algebraic eddy viscosity concept) that could improve the overall flowfield prediction. The present test flow case has been selected for two main reasons: 1) shock/boundary-layer interaction is an important phenomenon in many practical high-speed flows,[13] and 2) sufficiently detailed experimental measurements[14-16] are available for the 2-D compression ramp configuration.

The compression corner flows were simulated using the full 2-D mass-averaged Navier-Stokes equations[17] expressed in strong conservation form[18] and in general curvilinear coordinates. Several versions of the Baldwin-Lomax algebraic turbulence model were investigated, including the incorporation of the relaxation technique of Shang and Hankey.[19] The governing equations were solved in nearly orthogonal body-fitted grids[20] employing the implicit, approximate-factorization algorithm of Beam and Warming.[1]

Submitted May 16, 1983; presented as Paper 83-1697 at the AIAA 16th Fluid and Plasma Dynamics Conference, Danvers, Mass, July 12-14, 1983; revision received Oct. 28, 1983.

*Graduate Student, Dept. of Mechanical and Aerospace Engineering; presently, Visiting Scientist, Air Force Wright Aeronautical Lab., Wright Patterson AFB. Member AIAA.

†Associate Professor, Dept. of Mechanical and Aerospace Engineering. Member AIAA.

II. Method of Solution

Governing Equations and Turbulence Models

The governing equations are the full mean compressible Navier-Stokes equations in two dimensions using mass-averaged variables,[17] strong conservation form,[18] and general curvilinear coordinates. The fluid is assumed thermally and calorically perfect. The molecular dynamic viscosity μ is given by Sutherland's law. The molecular Prandtl number $Pr=0.73$ (for air) and the turbulent Prandtl number $Pr_t=0.9$.

Three different versions of an algebraic two-layer turbulent eddy viscosity model were employed in the present computations. The first turbulence model is that proposed by Baldwin and Lomax.[6] In the inner region the eddy viscosity is given by the Prandtl-Van Driest formulation

$$\epsilon_i=\rho(KYD)^2|\omega| \tag{1}$$

where ρ is the density, $|\omega|$ the magnitude of the vorticity, $K=0.40$ is von Kármán's constant, and Y is the normal distance from the wall. The Van Driest damping factor D is given by

$$D=1-\exp(-Y\sqrt{\rho_w|\tau_w|}/26\mu_w) \tag{2}$$

where τ_w is the wall shear stress. In the outer region, in order to eliminate the need of finding the boundary-layer edge, Baldwin and Lomax replaced Clauser's formulation by the following relation

$$\epsilon_0=\rho k C_{cp} F_{\text{wake}} F_{\text{kleb}} \tag{3}$$

where $k=0.0168$ is Clauser's constant and C_{cp} is an additional constant. The outer function F_{wake} is

$$F_{\text{wake}}=Y_{\max}F_{\max} \tag{4}$$

where $F_{\max}=\max(Y|\omega|D)$, and $Y_{\max}$ is the value of Y at which $F_{\max}$ occurs. The Klebanoff intermittency correction is given by

$$F_{\text{kleb}}=[1+5.5(C_{\text{kleb}}Y/Y_{\max})^6]^{-1} \tag{5}$$

where C_{kleb} is a constant. In the original Baldwin-Lomax model,[6] an alternate formulation, applicable to wake flows, was included in the expression for F_{wake}. Although this formulation has been employed in previous computations[6,7,11] of shock/boundary-layer interactions, it is the authors' opinion that its use is not justified for the present investigation, and, therefore, was not considered. The turbulent eddy viscosity is switched from the inner to the outer formulation at the location where $\epsilon_i>\epsilon_0$. Baldwin and Lomax suggested the values for $C_{cp}=1.6$ and $C_{\text{kleb}}=0.3$ based on a comparison with the Cebeci and Smith model[4] for equilibrium boundary layers at transonic speeds. In the present research, these constants were found to be dependent on the Mach number of the flow. It can be shown[21] that for an equilibrium incompressible ($M_\infty=0$) turbulent boundary layer, which obeys the wall/wake law,[22] the values $C_{cp}=1.2$ and $C_{\text{kleb}}=0.65$ are required in the Baldwin-Lomax model in order to match the Clauser-Klebanoff formulation. In addition, a series of flat plate near-adiabatic ($T_w/T_{\text{adiabatic}}=1.12$) turbulent boundary-layer computations at Mach 3.0 dictated the use of $C_{cp}=2.08$ for the present ramp calculations.[23]

The elimination of the need to determine the boundary-layer edge in the outer eddy viscosity formulation constitutes a major advantage of the Baldwin-Lomax model over the Cebeci-Smith model. This is only true, however, when the outer function $F=Y|\omega|D$ provides an unambiguous evaluation of the velocity scale $F_{\max}$ and the length scale $Y_{\max}$. For equilibrium turbulent boundary layers, as well as for transonic flow over an airfoil,[6] the outer function F typically displays a single well-defined extremum and the determination of $F_{\max}$ and $Y_{\max}$ is straightforward. For separated supersonic flow over a compression ramp, however, the present research indicates that F displays two peaks in the vicinity of separation. Similar behavior was observed by Baldwin and Lomax[6] for a 2-D oblique shock/turbulent boundary-layer interaction. Since the values of $Y_{\max}$ associated with each one of these extrema may differ by one order of magnitude, the selection of the peak closer to the wall (at the streamwise locations where it represents the absolute maximum) results in an abrupt, unphysical reduction in the computed outer eddy viscosity. An additional problem in the Baldwin-Lomax model (for both the inner and outer formulation) may be caused by the vanishing of the Van Driest damping factor D at the locations where τ_w approaches zero (i.e., near separation and reattachment in 2-D flows). The small values of D result in an unphysical reduction of the computed eddy viscosity. This effect is found to be more pronounced for the inner eddy viscosity in the vicinity of reattachment, and in some cases (see Sec. III) can prevent the flowfield from achieving a fully steady state in this region.

In order to avoid the above difficulties, a second turbulence model, referred to subsequently as the modified Baldwin-Lomax model, was employed. This new version incorporates two modifications, namely, 1) at the locations where F displays two peaks, the values of $F_{\max}$ and $Y_{\max}$ are obtained from the extremum farthest from the wall (outer peak), and 2) in the Van Driest damping factor [Eq. (2)], the local value of the total shear stress (defined in terms of the velocity component parallel to the wall) is used in place of τ_w.

The third turbulence model incorporates the relaxation technique of Shang and Hankey[19] in an attempt to account for upstream turbulence history effects. The relaxation eddy viscosity ϵ (for both the inner and the outer formulation) is given by

$$\epsilon=\epsilon_{\text{eq}}+(\epsilon_{\text{upst}}-\epsilon_{\text{eq}})\exp[-(X-X_0)/\lambda] \qquad X\geq X_0 \tag{6}$$

where ϵ_{eq} is obtained from the modified Baldwin-Lomax model and ϵ_{upst} denotes the value of the eddy viscosity at the upstream location X_0 where the surface pressure rise begins. A relaxation length λ equal to the incoming boundary-layer thickness δ_0 was employed in the present computations. The determination of the value of the relaxation length is discussed in Sec. III.

Computational Domain and Boundary Conditions

The shape of the computational domain is shown in Fig. 1. The inflow boundary was located ahead of the corner in a region of no upstream influence. The outflow boundary was placed sufficiently far from the corner, in a region of small streamwise flow gradients. The height of the computational domain (3-4 δ_0) was chosen so as to obtain freestream conditions along the upper boundary and to ensure the emergence of the shock through the downstream boundary.

On the solid surface, the nonslip, isothermal conditions $u=v=0$ and $T=T_w$ were applied along with a boundary condition for the pressure derived from the normal component of the momentum equation.[21] For the freestream boundary, a no-reflection condition,[24] suitable for supersonic flow, was prescribed. Along the outflow boundary, the conventional extrapolation condition $\partial/\partial\xi=0$ was employed. The upstream boundary conditions were obtained by calculating the development of a flat plate turbulent boundary layer up to the locations where the computed momentum thickness θ matched the experimental value. At the same locations, the computed and measured velocity, skin friction and displacement thickness were also compared and found in very good agreement. For instance, at the matching station

where $Re_\theta = 8.2 \times 10^4$, the computed and measured skin-friction coefficient c_f are 1.02×10^{-3} and 1.00×10^{-3}, respectively. The value of c_f predicted by the Van Driest II theory and the von Kármán-Schoenherr equation[25] is 1.04×10^{-3}. At the same station, the computed displacement thickness δ^* is essentially equal to the experimental value (0.66 cm). Excellent agreement was also found[21] between the computed and measured velocity profiles and the law of the wall.[22]

The computational grids were generated by the numerical procedure of Ref. 20. A nonuniform mesh spacing was used in both coordinate directions in order to provide sufficient resolution of the turbulent boundary layer and the interaction region. In the direction normal to the surface, the grid points were distributed using a combination of geometrically stretched and uniform spacing. The normal spacing at the wall was chosen in order to resolve the viscous sublayer, and satisfied the requirement $\Delta Y^+_{\min} \leq 2.5$ at all locations. The typical number of grid points within the boundary layer was 25 to 30. The streamwise mesh spacing in the interaction region ranged from 0.027 δ_0 for the 8-deg ramp to 0.077 δ_0 (for the 24-deg ramp). The maximum streamwise spacing (outside the interaction region) was always less than 0.6 δ_0.

Numerical Algorithm

The governing equations were solved using the implicit, approximate-factorization algorithm of Beam and Warming.[1] This scheme was formulated employing Euler implicit time-differencing and second-order, centered approximations for the spatial derivatives. The boundary conditions were implemented in the explicit or lagged approach described by Steger.[26] Fourth-order explicit damping terms, required for the smoothing of the embedded shocks, were prescribed according to the procedure of Ref. 27. The developed Navier-Stokes computer code was extensively validated,[21] with excellent results, for several test cases including inviscid shocked flows, laminar and turbulent boundary layers, and laminar shock/boundary-layer interactions.

Since the compression ramp flowfields are obtained by time integration of the unsteady Navier-Stokes equations until a steady state is reached, considerable care was exercised in ensuring convergence. Separated interactions were run for physical times of up to $10t_c$, where t_c is the time required for a fluid parcel in the inviscid region to travel from the upstream to the downstream end of the mesh. The flowfields were assumed converged when the maximum relative variation of the flow variables over $1t_c$ were less than 1.0%. It should be noted that, while changes of order 1.0% occur at a few mesh points (in regions of shock smearing), the relative changes were much smaller at most locations. The corresponding average variations over $1t_c$ were typically less than 0.05%.

III. Results and Discussion

Figure 1 illustrates the compression corner geometry employed in the present evaluation of the Baldwin-Lomax model. An extensive experimental study of this flow configuration, for a nominal Mach number $M_\infty = 2.9$, has been conducted in recent years.[14-16] The available experimental date base[14] may be divided into two major categories: 1) surface and mean flowfield data for four corner angles ($\alpha = 8$, 16, 20, and 24 deg) at a fixed Reynolds number $Re_{\delta_0} = 1.6 \times 10^6$, and 2) surface data (including wall pressure and separation and reattachment locations) for a fixed ramp angle of 20 deg at four different Reynolds numbers ($Re_{\delta_0} = 0.76 \times 10^6$, 3.4×10^6, 5.6×10^6, and 7.7×10^6). The first category includes measurements of surface pressure; skin friction; and velocity, Mach number, and static pressure profiles at nine streamwise stations for each ramp angle. These flowfields encompass nominally attached (8-deg ramp), as well as fully separated (20- and 24-deg ramps) interactions. Computations were performed for all eight of the above experimental cases. For the first category (i.e., variable ramp angle), the different versions of the algebraic turbulence model were employed. For the second category (i.e., variable Re_{δ_0}), only the relaxation model was applied. A detailed comparison of the computed flowfields and the experimental data was performed; however, only the most significant results are presented below. Reference 21 contains a more extensive comparison along with the details of all computations.

Results for Variable Ramp Angle

Results for 16-deg Ramp

The 16-deg ramp flowfield was computed using each of the versions of the turbulence model. This compression corner flow constitutes, according to the experiments, an incipiently separated interaction. The computed and measured surface pressure is shown in Fig. 2. The results for the original Baldwin-Lomax and relaxation models are in close agreement

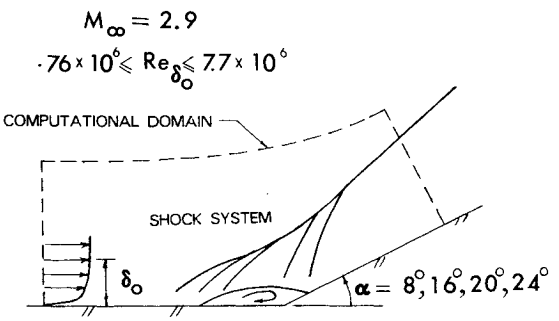

Fig. 1 Flow configuration and computational domain.

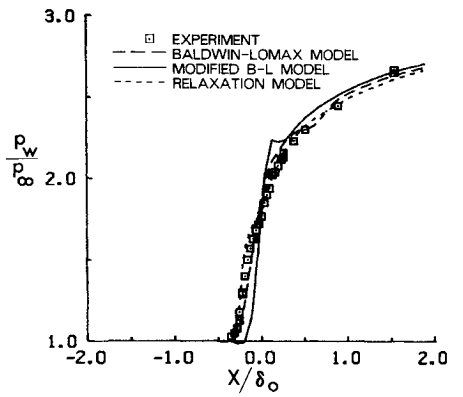

Fig. 2 Surface pressure distribution for 16-deg ramp.

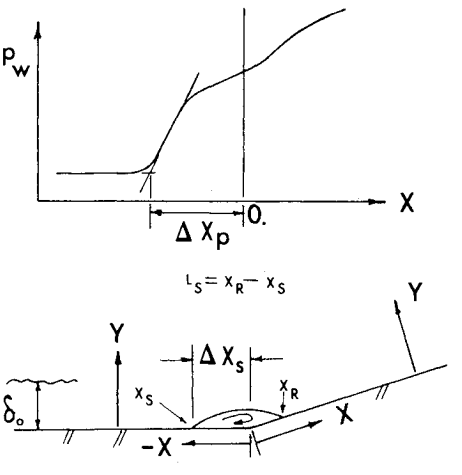

Fig. 3 Definition of interaction geometric distances.

with each other and with the experimental data. However, the computed surface pressure obtained with the modified model displays an insufficient upstream propagation ΔX_p (see Fig. 3 for the definition of geometric distances), similar to the results of Shang and Hankey[19] and Horstman et al.,[28] who employed the Cebeci-Smith turbulence model.

The skin-friction results are presented in Fig. 4. All calculations predict the existence of a separated region, which is not displayed by the experiments. The original Baldwin-Lomax and relaxation models are in reasonably good agreement with the experiment in the region of sharply decreasing c_f. However, both models seriously underpredict the skin-friction values in this recovery region (i.e., downstream of reattachment). Also, the computed separation-to-reattachment lengths are too large. The modified model provides substantial improvement in this regard. Downstream of attachment, however, all models approach the same skin-friction level which is significantly below the measured value. This behavior is similar to previous computations using algebraic eddy viscosity models.[28]

The computed and experimental velocity profiles at three stations (upstream, at the corner, and downstream of the interaction) are shown in Fig. 5. The original and relaxation models give slightly better results upstream and at the corner (first two profiles). Downstream of reattachment, all three models result in a velocity profile that displays an insufficient recovery or "filling out" near the wall. This observation is consistent with the underprediction of skin friction discussed above.

Figure 6 shows the evolution of the outer function $F = Y|\omega|D$ across the interaction, for the calculation with the original Baldwin-Lomax model. The corresponding value of Y_{max}, and the maximum value of ϵ_0 at each streamwise station are given in Figs. 7 and 8. Upstream of the interaction ($X/\delta_0 = -1.1$), F displays a single, well-defined peak. Immediately before the separation point ($X/\delta_0 = -0.27$), F exhibits two distinct extrema (referred to subsequently as the inner and outer peak). At this location the outer peak, which represents the absolute maximum, is still chosen by the model to compute F_{max} and Y_{max}. Downstream of separation ($X/\delta_0 = -0.19$), the inner peak, which is very close to the wall, exceeds the outer one, and Y_{max} abruptly decreases by one order of magnitude (Fig. 7). Despite the increase in F_{max}, a net sudden drop in F_{wake} occurs. This reduction in F_{wake}, combined with the effect of Y_{max} in the Klebanoff intermittency correction [Eq. (5)], produces a sharp decrease in the computed outer eddy viscosity (Fig. 8). As Fig. 6 indicates, the outer peak disappears further downstream, and the inner peak moves away from the surface to a new equilibrium position. These large streamwise variations in the computed length scale Y_{max} are unphysical and constitute a major deficiency of the original Baldwin-Lomax model for

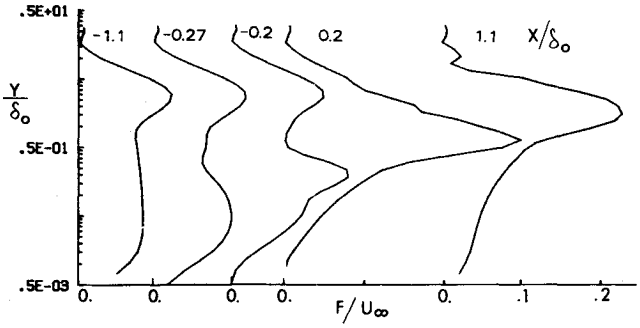

Fig. 6 Evolution of the Baldwin-Lomax outer eddy viscosity function $F(Y)$ across 16-deg ramp interaction.

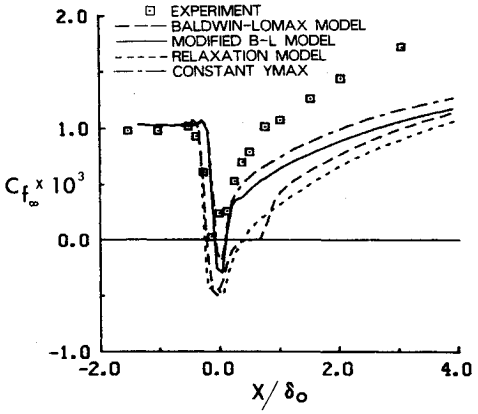

Fig. 4 Skin-friction coefficient for 16-deg ramp.

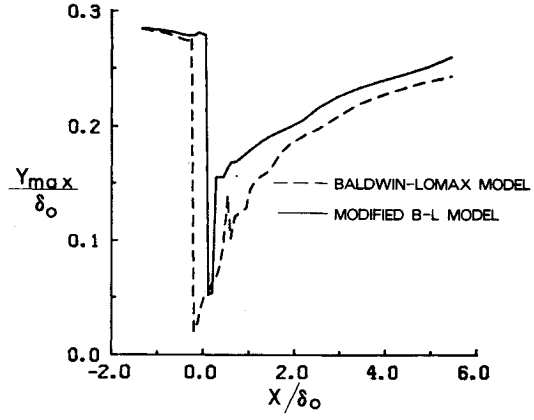

Fig. 7 Variation of Y_{max} across 16-deg ramp interaction.

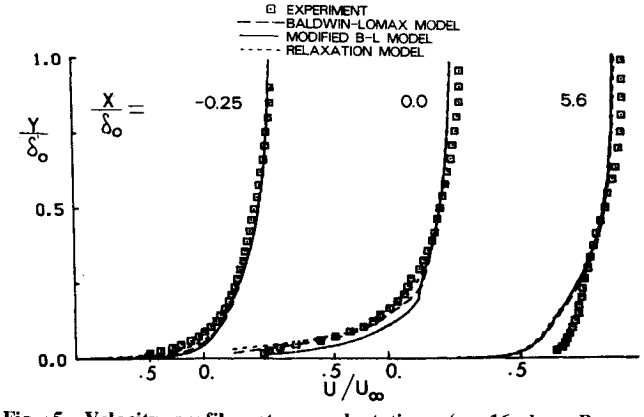

Fig. 5 Velocity profiles at several stations ($\alpha = 16$ deg, $Re_{\delta_0} = 1.6 \times 10^6$).

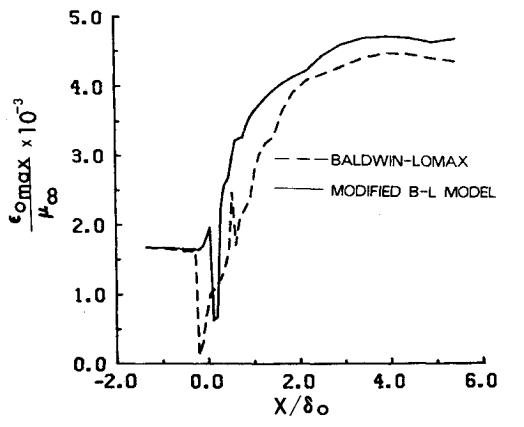

Fig. 8 Variation of $\epsilon_{\theta_{max}}$ across 16-deg ramp interaction.

the prediction of supersonic shock/boundary-layer interactions. Similar problems were encountered by Baldwin and Lomax[6] in the computation of a 2-D oblique shock interaction, and by Knight[23] in a 3-D interaction.

The behavior of the outer function F in the interaction region for the modified Baldwin-Lomax model is similar to that described above. The corresponding value of Y_{max} and ϵ_{0max} are also shown in Figs. 7 and 8. Since in the modified model the outer peak is always selected, an abrupt decrease in Y_{max} and ϵ_{0max} still occurs at the streamwise location where the outer peak in F disappears.

For the 16-deg ramp computation using the original Baldwin-Lomax model, a fully steady-state solution could not be achieved in a small region close to the wall in the immediate vicinity of reattachment. In this region the flow variables exhibited bounded oscillations in time. This problem is apparently associated with the very low values of the computed inner eddy viscosity, cased by the Van Driest damping factor D [Eq. (2)] approaching zero in the reattachment region. This difficulty was overcome in the modified version of the model by employing the local total shear stress in the evaluation of D.

In order to investigate the effects of the length scale Y_{max}, an additional computation was performed for the 16-deg ramp utilizing the modified Baldwin-Lomax model with a constant or "frozen" value of Y_{max} throughout the flowfield. The computed surface pressure was essentially identical to the results for the modified model. The computed skin-friction coefficient, shown in Fig. 4, gave only a slight improvement in the recovery region. The velocity profile at the downstream station $X/\delta_0 = 5.4$ (not shown) was very close to the previous results (Fig. 5), and again failed to predict the rapid recovery of the boundary layer downstream. This calculation indicates that the computed flowfield in the recovery region is not very sensitive to changes in the outer eddy viscosity.

Results for 20-deg Ramp

The 20-deg compression ramp was simulated using the three different versions of the turbulence model. This case represents, according to the experiments, a fully separated interaction. The computed and measured surface pressure is shown in Fig. 9. The results for the modified Baldwin-Lomax model significantly underpredict the extent of upstream propagation and do not display the pressure "plateau" observed in the experiments. The use of relaxation, with a relaxation length $\lambda = \delta_0$, substantially improves the wall pressure prediction and gives the correct upstream influence. However, the computed pressure plateau is more pronounced than in the experiments. The computed pressure for the original model falls between the results for the modified and relaxation models. The skin-friction results are shown in Fig. 10. The relaxation and original models provide a better agreement with the experiment upstream of separation. Downstream of reattachment, all models seriously underpredict the recovery of the boundary layer. The computed separation-to-reattachment length is too large, although the modified model does slightly better in this respect.

Figure 11 shows the computed and measured velocity profiles at several streamwise locations. The relaxation model gives some improvement in the computed velocity for the first part of the interaction. This is consistent with the better prediction of upstream propagation discussed above. Downstream of reattachment, all models fail to predict the rapid recovery of the velocity near the wall. The results for the static pressure are given in Fig. 12. In the interaction region, the relaxation model displays the best comparison with the experiment. The measured static pressure profiles downstream of reattachment exhibit a normal gradient near the

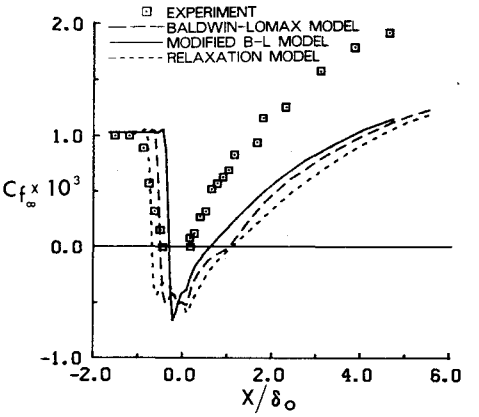

Fig. 10 Skin-friction coefficient for 20-deg ramp.

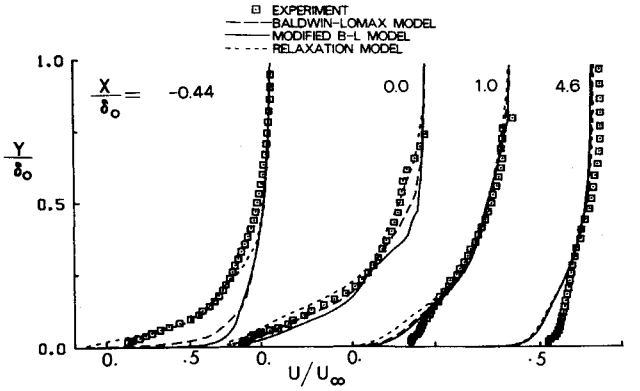

Fig. 11 Velocity profiles at several stations ($\alpha = 20$ deg, $Re_{\delta_0} = 1.6 \times 10^6$).

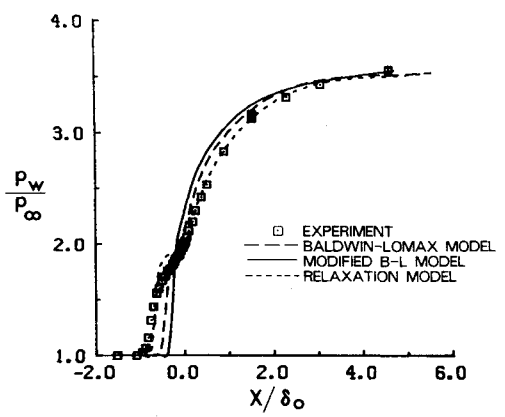

Fig. 9 Surface pressure distribution for 20-deg ramp.

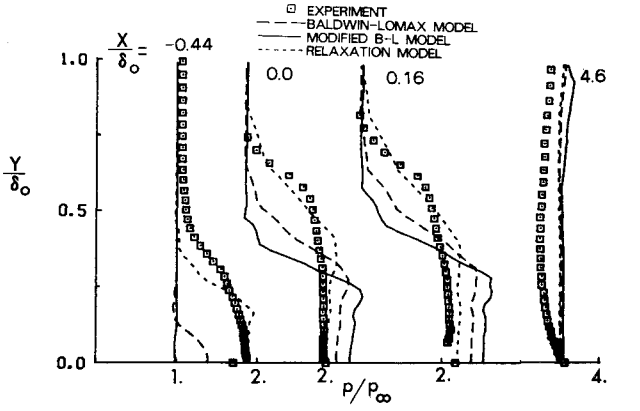

Fig. 12 Static pressure profiles at several stations ($\alpha = 20$ deg, $Re_{\delta_0} = 1.6 \times 10^6$).

wall, which is not duplicated in the computations. This observation also applies to the 16- and 24-deg ramp flows.

Results for 24-deg Ramp

This fully separated compression corner interaction was simulated using the modified Baldwin-Lomax and relaxation turbulence models. The comparison of computed and experimental results, contained in Figs. 13-15, exhibits the same characteristics observed for the 20-deg ramp. As compared with the modified model, the relaxation model (with $\lambda=\delta_0$) provides a marked improvement in the prediction of surface pressure distribution (Fig. 13), including the pressure plateau level and the extent of upstream influence. This agreement dictated the use of $\lambda=\delta_0$ in the present research. This value of λ was also found by Horstman et al.[28] to predict ΔX_p reasonably well. On the other hand, Shang and Hankey[19] required a value of $\lambda=10\delta_0$ in their compression corner calculations. This will be discussed in more detail below. The use of relaxation also results in a closer agreement with the measured skin friction ahead of separation (Fig. 14). Both models, however, overpredict the length of the separation region, and do not provide the correct skin-friction level downstream of reattachment. The higher values of c_f obtained by Baldwin and Lomax[6] for the 24-deg ramp case are in contradiction with the present results and those of Ref. 28.

Upstream of the corner, the relaxation model produces again an improvement in the predicted velocity profiles (Fig. 15). Downstream of reattachment, both models fail to simulate the rapid recovery of the boundary layer near the wall.

In order to examine the effects of the relaxation length on the computed flowfield, the 24-deg ramp flow was also calculated using a "frozen" eddy viscosity model. The term "frozen" denotes that the eddy viscosity profile upstream of the interaction was employed at all streamwise locations [i.e., $\lambda=\infty$ in Eq. (6)]. The computation was run for approximately three characteristic times, at which point the extent of upstream propagation ΔX_p had increased by almost 100%, as compared with the previous results for the relaxation model with $\lambda=\delta_0$. Results by Horstman et al.[28] for the same flow conditions indicated an increase of up to 50% in ΔX_p when λ was changed from 1 δ_0 to 5 δ_0. On the other hand, computations by Shang and Hankey[19] for a 25-deg ramp (with M_∞-2.96 and $Re_{\delta_0}=1.4\times10^5$) employing a frozen and a relaxation ($\lambda=10\delta_0$) model, did not exhibit this drastic difference in ΔX_p. The use of $\lambda=10\delta_0$ is then expected to produce a gross overprediction of the upstream influence for the present compression corner flow. Since essentially the same baseline turbulence model (namely Cebeci-Smith[4]) was used in Refs. 19 and 28, the discrepancy in the value of λ, required to match the experimental pressure, is probably due to the difference in the flow Reynolds number Re_{δ_0}. In fact, the measured separation-to-reattachment length for the present 24-deg ramp flow is $1.7\delta_0$, while the corresponding length for the 25-deg ramp considered in Ref. 19 is approximately 8 δ_0. This could be interpreted as a dependence of λ on the extent of the interaction, which for a given geometry is a function of the flow parameters (Re_{δ_0} and M_∞). This variation of the relaxation length λ (which is intended to represent the lagged response of the turbulent stress to sudden mean flow gradients) is perhaps reasonable since for separated shock/boundary-layer interactions large increases in the Reynolds stress are observed[29] before the reattachment location.

Results for Variable Reynolds Number

Since the previous results for variable ramp angle indicated that the use of relaxation provides some improvement in the prediction of the interaction upstream influence, it is of in-

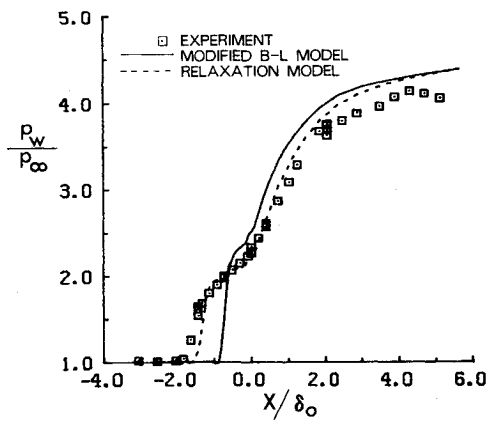

Fig. 13 Surface pressure distribution for 24-deg ramp.

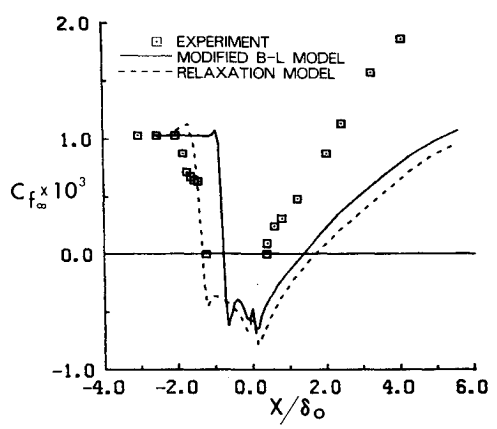

Fig. 14 Skin-friction coefficient for 24-deg ramp.

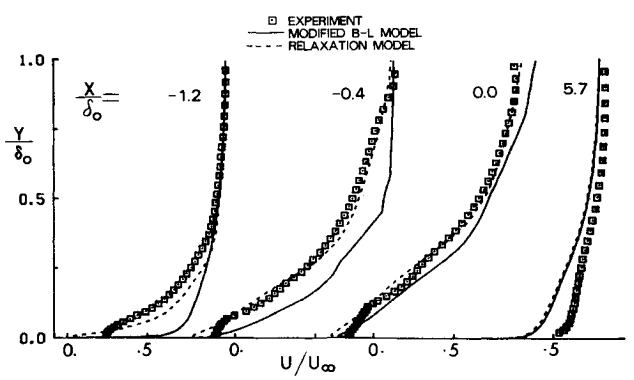

Fig. 15 Velocity profiles at several stations ($\alpha=24$ deg, $Re_{\delta_0}=1.6\times10^6$).

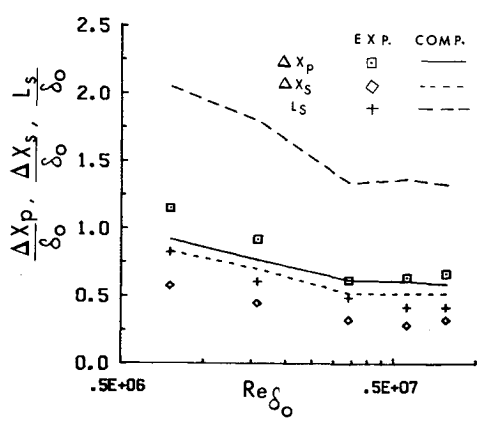

Fig. 16 Effect of Re_{δ_0} on ΔX_p, ΔX_s, and L_s ($\alpha=20$ deg).

terest to evaluate the relaxation model for the case of variable Reynolds number. For this purpose, several calculations were performed for a 20-deg ramp over the Reynolds number range $0.76\times10^6 \le Re_{\delta_0} \le 7.75\times10^6$, using the relaxation turbulence model only.

In order to illustrate the effects of Reynolds number on the interaction, the values of ΔX_p, ΔX_s (see Fig. 3 for definitions) and the separation-to-reattachment length L_s are presented as functions of Re_{δ_0} in Fig. 16. Although the computed results for ΔX_p, ΔX_s, and L_s exhibit the correct Reynolds number trend, only the upstream pressure influence ΔX_p is predicted with reasonable accuracy (see Refs. 16 and 28 for the scatter of the experimental data). The distance from the separation location to the corner ΔX_s as well as the overall separation length L_s are consistently overpredicted. The above observations are in agreement with the results of Ref. 28. The relaxation model (with a constant relaxation length $\lambda=\delta_0$) is capable of predicting the upstream pressure influence with reasonable accuracy over the entire Reynolds number range investigated.

IV. Conclusions

A critical evaluation of the algebraic turbulence model of Baldwin and Lomax was performed for the case of 2-D shock/boundary-layer interactions induced by compression corners. Three different versions of this algebraic eddy viscosity model were investigated, including the incorporation of relaxation.[19] A detailed comparison of the computed flowfields with the available experimental data[14] was performed, and the capabilities and deficiencies of the turbulence models were identified.

Regarding the characteristics of the Baldwin-Lomax model for 2-D supersonic interactions, the following specific conclusions can be made:

1) The constants C_{cp} and C_{kleb}, appearing in the Baldwin-Lomax outer formulation, were found to be dependent on the flow Mach number. These constants vary by a factor of two over the Mach number range $0\le M_\infty \le 3.0$, and therefore need to be adjusted accordingly.

2) The Baldwin-Lomax outer function ($F=Y|\omega|D$) is not suitable for the determination of the length scale in the separation region of the interactions investigated. This is due to the appearance, near separation, of a double peak in $F(Y)$ which results in an abrupt (unphysical) decrease in the computed length scale. This behavior constitutes a major deficiency of the model for supersonic interactions, and could perhaps be eliminated by the use of a different outer function. In addition, for an incipiently separated interaction, the small values of the eddy viscosity near the reattachment location (caused by the vanishing of the Van Driest damping factor) can prevent the solution from achieving a fully steady state.

The above difficulties can be partially overcome by using the local total shear stress in the Van Driest damping term and by the selection of the outermost peak of $F(Y)$ in the computation of the length scale. These modifications provide a better flow prediction near reattachment.

3) Computations with the original and modified Baldwin-Lomax models exhibit an insufficient upstream propagation, caused by the inability of the models to reproduce the lagged response of the turbulence structure to the sudden adverse pressure gradient. Significant improvement in the flowfield prediction upstream of the corner can be obtained with the use of relaxation. A relaxation length equal to the incoming boundary-layer thickness was found to be suitable for the range of Reynolds numbers and ramp angles considered. This value, however, is one-tenth of that suggested by Shang and Hankey[19] and is expected to depend on the extent of the interaction.

4) All of the turbulence models tested here fail to predict the rapid recovery of the boundary layer downstream of reattachment. This is due to the inability of the models to simulate the observed[29-33] amplification of the turbulence fluctuations across a shock/boundary-layer interaction. This deficiency would lead to a rather poor prediction of flows with multiple interactions, and means of improving the present results have not yet been found. The fact that downstream of the interaction, the mean velocity profile rapidly approaches its equilibrium shape, while the enhanced turbulence fluctuations relax very slowly toward equilibrium,[30-32] points out the inadequacy of the algebraic eddy viscosity concept for these complex flowfields.

Acknowledgments

The authors gratefully acknowledge many helpful and stimulating discussions with S. Bogdonoff, D. Dolling, G. Settles, and L. Smits. This research was supported by the Air Force Office of Scientific Research under AFOSR Grant 82-0040, monitored by J. Wilson. Initial development of the numerical algorithm was supported by the Air Force Flight Dynamics Laboratory-Air Force Wright Aeronautical Laboratories under AFOSR Grant 80-0072, monitored by J. Mace.

References

[1] Beam, R. and Warming, R., "An Implicit Factored Scheme for the Compressible Navier-Stokes Equations," *AIAA Journal*, Vol. 16, April 1978, pp. 393-402.

[2] MacCormack, R. W., "A Numerical Method for Solving the Equations of Compressible Viscous Flow," AIAA Paper 81-0110, 1981.

[3] Thompson, J. F., Warsi, Z. U. A., and Mastin, C. W., "Boundary Fitted Coordinate Systems for Numerical Solution of Partial Differential Equations—A Review," *Journal of Computational Physics*, Vol. 47, 1982, pp. 1-108.

[4] Cebeci, T. and Smith, A. M. O., *Analysis of Turbulent Boundary Layers*, Academic Press, New York, 1974.

[5] Hung, C. M. and MacCormack, R.W., "Numerical Simulation of Supersonic and Hypersonic Turbulent Compression Corner Flows," *AIAA Journal*, Vol. 15, March 1977, pp. 410-416.

[6] Baldwin, B. and Lomax, H., "Thin Layer Approximation and Algebraic Model for Separated Turbulent Flows," AIAA Paper 78-257, 1978.

[7] Hung, C.M. and Chausee, D. S., "Computation of Supersonic Turbulent Flows Over an Inclined Ogive-Cylinder-Flare," AIAA Paper 80-1410, 1980.

[8] Deiwert, G. S., "Numerical Simulation of Three-Dimensional Boattail Afterbody Flow Field," AIAA Paper 80-1347, 1980.

[9] Kutler, P., Chakravarthy, S. R., and Lombard, C. K., "Supersonic Flow Over Ablated Nosetips Using an Unsteady, Implicit Numerical Procedure," AIAA Paper 78-213, 1978.

[10] Steger, J., Pulliam, T., and Chima, R., "An Implicit Finite Difference Code for Inviscid and Viscous Cascade Flows," AIAA Paper 80-1427, 1980.

[11] Hung, C. M., *1980-1981 AFOSR-HTTM-STANFORD Conference on Complex Turbulent Flows*, Vol. III, edited by S. J. Kline et al., 1982, Thermosciences Div., Mechanical Engineering Department, Stanford Univ., pp. 1283-84 and 1372-74.

[12] Degani, D. and Schiff, L. B., "Computation of Supersonic Viscous Flows Around Pointed Bodies at Large Incidence," AIAA Paper 83-0034, 1983.

[13] Korkegi, R. H., "Survey of Viscous Interactions Associated with High Mach Number Flight," *AIAA Journal*, Vol. 9, May 1971, pp.771-784.

[14] Settles, G., Gilbert, R., and Bogdonoff, A., "Data Compilation for Shock Wave/Turbulent Boundary Layer Interaction Experiments on Two-Dimensional Compression Corners," Dept. of Aerospace and Mechanical Engineering, Princeton University, Princeton, N. J., Rept. MAE-1489, 1980.

[15] Settles, G., Fitzpatrick, T., and Bogdonoff, S., "Detailed Study of Attached and Separated Compression Corner Flowfields in High Reynolds Number Supersonic Flow," *AIAA Journal*, Vol. 17, 1979, pp. 579-585.

[16] Settles, G., Bogdonoff, S., and Vas, I.E., "Incipient Separation of a Supersonic Turbulent Boundary Layer at High Reynolds Numbers," *AIAA Journal*, Vol. 14, Jan. 1976, pp. 50-56.

[17] Rubesin, M. and Rose, W., "The Turbulent Mean-Flow, Reynolds-Stress and Heat-Flux Equations in Mass Averaged Dependent Variables," NASA TMX-62248, March 1973.

[18] Pulliam, T. and Steger, J., "Implicit Finite-Difference Simulations of Three-Dimensional Compressible Flow," *AIAA Journal,* Vol. 18, Feb. 1980, pp. 159-167.

[19] Shang, J. and Hankey, W. L., Jr., "Numerical Solution for Supersonic Turbulent Flow Over a Compression Ramp," *AIAA Journal,* Vol. 13, Oct. 1975, pp. 1368-1374.

[20] Visbal, M. and Knight, D. D., "Generation of Orthogonal and Nearly Orthogonal Coordinates with Grid Control Near Boundaries," *AIAA Journal,* Vol. 20, March 1982, pp. 305-306.

[21] Visbal, M., "Numerical Simulation of Shock/Turbulent Boundary Layer Interactions Over 2-D Compression Corners," Ph.D. Thesis, Dept. of Mechanical and Aerospace Engineering, Rutgers University, New Jersey, Oct. 1983.

[22] Sun, C.-C. and Childs, M. E., "Wall-Wake Velocity Profile for Compressible Nonadiabatic Flows," *AIAA Journal,* Vol. 14, June 1976, pp. 820-822.

[23] Knight, D. D., "A Hybrid Explicit-Implicit Numerical Algorithm for the Three-Dimensional Compressible Navier-Stokes Equations," AIAA Paper 83-0223, 1983

[24] Knight, D. D., "Calculation of High Speed Inlet Flows Using the Navier-Stokes Equations," AFFDL-TR-79-3130, Vol. I, 1980.

[25] Hopkins, E. and Inouye, M., "An Evaluation of Theories for Predicting Turbulent Skin Friction and Heat Transfer on Flat Plates at Supersonic and Hypersonic Mach Numbers," *AIAA Journal,* Vol. 9, June 1971, pp. 993-1003.

[26] Steger, J. L., "Implicit Finite-Difference Simulation of Flow About Arbitrary Geometries with Application to Airfoils," AIAA Paper 77-665, 1977.

[27] Thomas, P. D., "Boundary Conditions and Conservative Smoothing Operators for Implicit Numerical Solutions to the Compressible Navier-Stokes Equations," LMSC-D630729, 1978.

[28] Horstman, C., Hung, C., Settles, G., Vas, I., and Bogdonoff, S., "Reynolds Number Effects on Shock-Wave Turbulent Boundary-Layer Interaction—A Comparison of Numerical and Experimental Results," AIAA Paper 77-42, 1977.

[29] Delery, J. M., "Experimental Investigation of Turbulence Properties in Transonic Shock/Boundary-Layer Interactions," *AIAA Journal,* Vol. 21, Feb. 1983, pp. 180-185.

[30] Settles, G. S., Baca, B. K., Williams, D. R., and Bogdonoff, S. M., "A Study of Reattachment of a Free Shear Layer in Compressible Turbulent Flow," AIAA Paper 80-1408, 1980.

[31] Rose, W. C., "The Behavior of a Compressible Turbulent Boundary Layer in a Shock-Wave-Induced Adverse Pressure Gradient," NASA TN D-7092, 1973.

[32] Hayakawa, K., Smits, A. J., and Bogdonoff, S. M., "Turbulence Measurements in a Compressible Reattaching Shear Layer," AIAA Paper 83-0299, 1983.

[33] Hayakawa, K., Smits, A.J., and Bogdonoff, S. M., "Hot-Wire Investigation of an Unseparated Shock-Wave/Turbulent Boundary Layer Interaction," AIAA Paper 82-0985, 1982.